High Magnetic Field X-ray Magnetic Circular Dichroism in Valence Fluctuating Compounds

Institute for Solid State Physics, University of Tokyo
Kashiwa, Chiba 277-8581, JAPAN

Yasuhiro H. MATSUDA

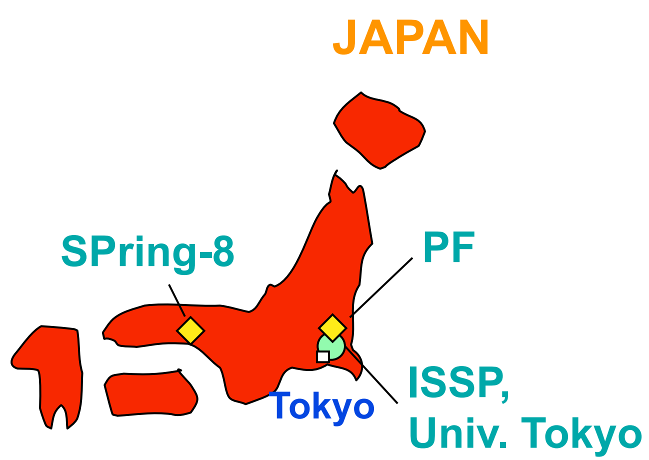

Main Collaborators

Hiroyuki NOJIRI (IMR, Tohoku Univ.)
Zhongwen OUYANG (IMR, Tohoku Univ. →HUST, China)
Toshiya INAMI (JAEA / SPring-8)
Kenji OHWADA (JAEA / SPring-8)
Jim-Long HER (ISSP, Univ. Tokyo)

Outline

1. Introduction
   Why X-ray experiments in high magnetic fields ?

2. A compact capacitor bank and a mini-magnet
   High field X-ray diffraction and X-ray absorption spectroscopy

3. XMCD of valence fluctuating compounds at the SPring-8
   $EuNi_2(Si_{1-x}Ge_x)_2$, $EuNi_2P_2$, ($YbInCu_4$)

4. High-magnetic-filed DXAFS system at the Photon Factory
   $Pr_{0.6}Ca_{0.4}MnO_3$

High magnetic fields

Zeeman splitting
Landau quantization
Wave function shrinkage

Phase transition
Quantum Phenomena

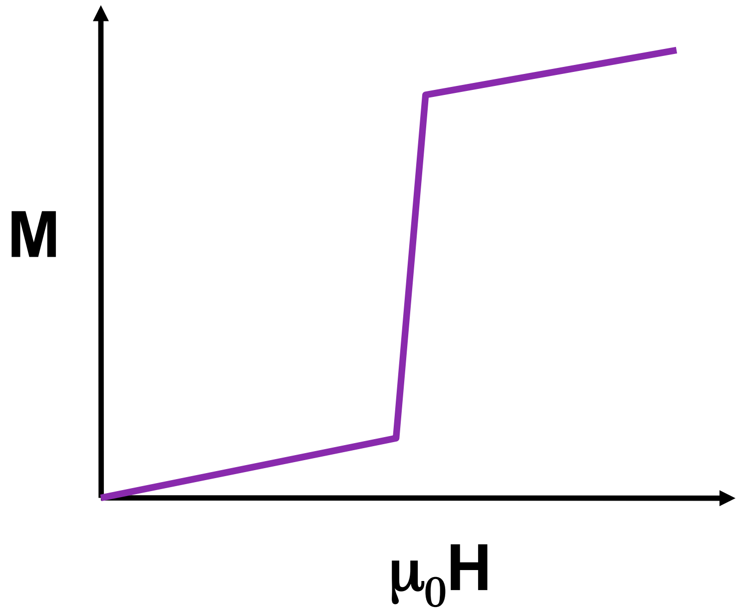

Microscopic Probe

Synchrotron X-rays

Crystal Structure
Electronic States

Diffraction
Spectroscopy

DC superconducting magnet ; B_{max} =15 T

We have many interesting phenomena in **40 T** range.

Field-induced superconductivity

λ-(BETS)$_2$FeCl$_4$

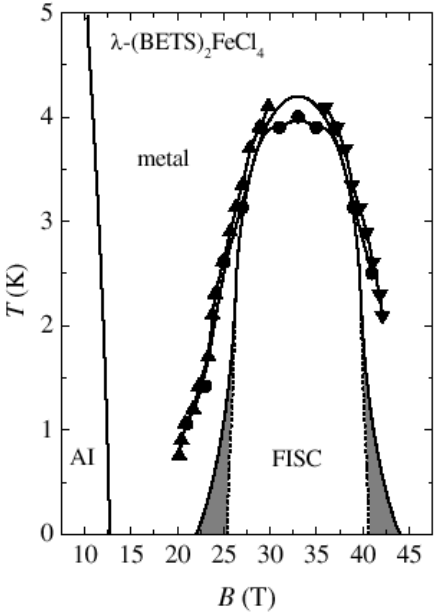

Balicas *et al.*, *Phys. Rev. Lett.* **87** (2001) 067002

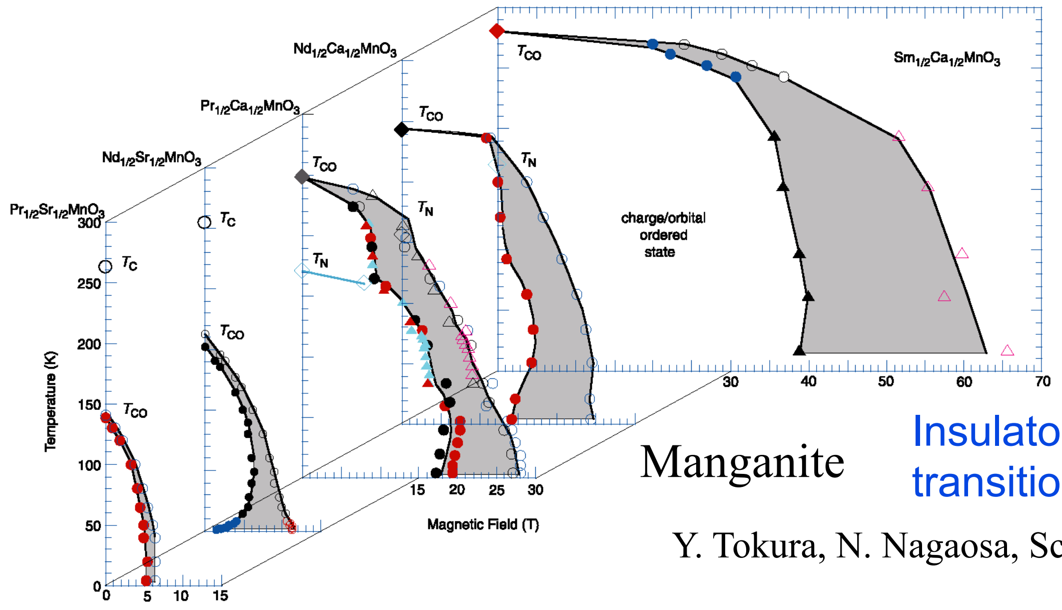

Manganite

Insulator-Metal transitions

Y. Tokura, N. Nagaosa, Science (2000)

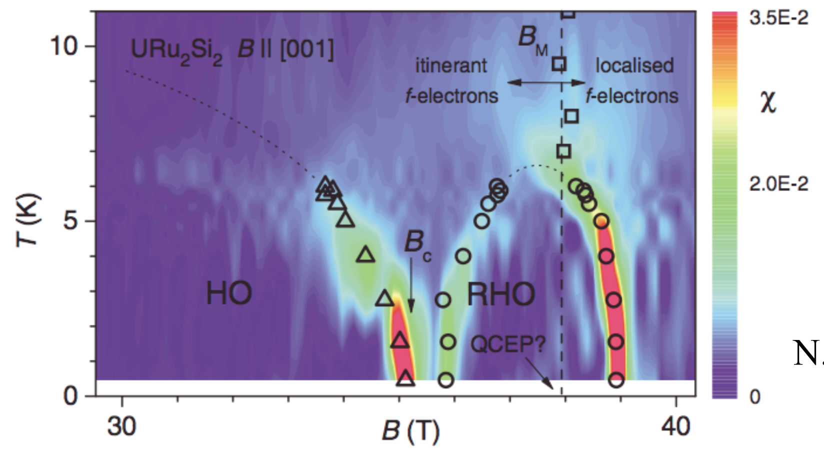

Quantum phase transition

URu$_2$Si$_2$

N. Harrison et al., PRL 90 (2003)

Miniature Pulsed Magnet and Portable Capacitor Bank

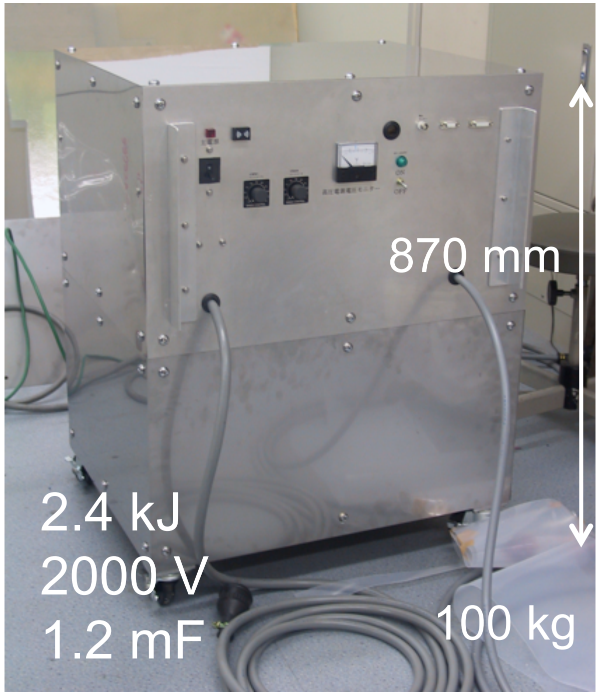

Small Energy

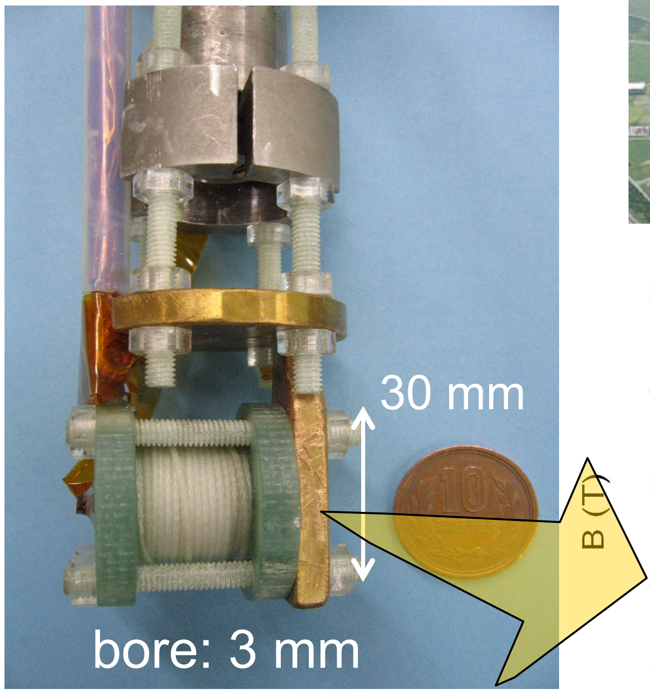

Small Space

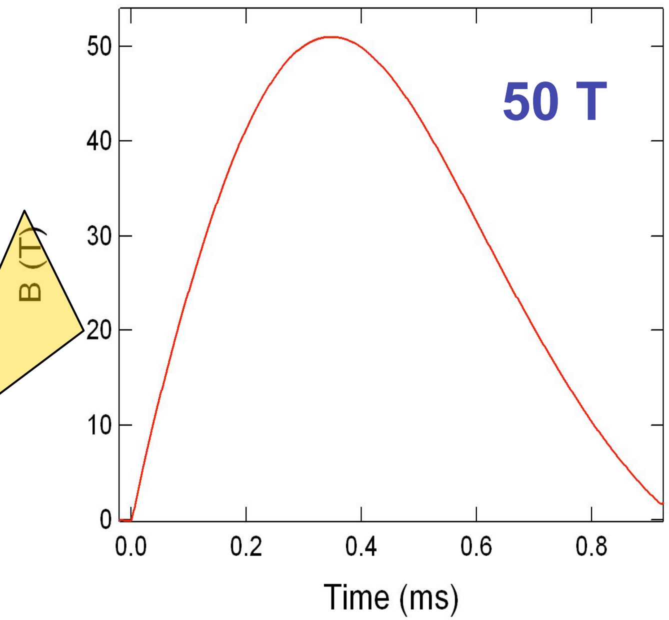

High Magnetic Field

Y. H. Matsuda et al., *Physica B* **346-347** (2004) 519-523.

Y. H. Matsuda et al., *Nuclear Instruments and Methods in Physics Research A* **528** (2004) 632-635.

High Magnetic Field Experiments at SPring-8

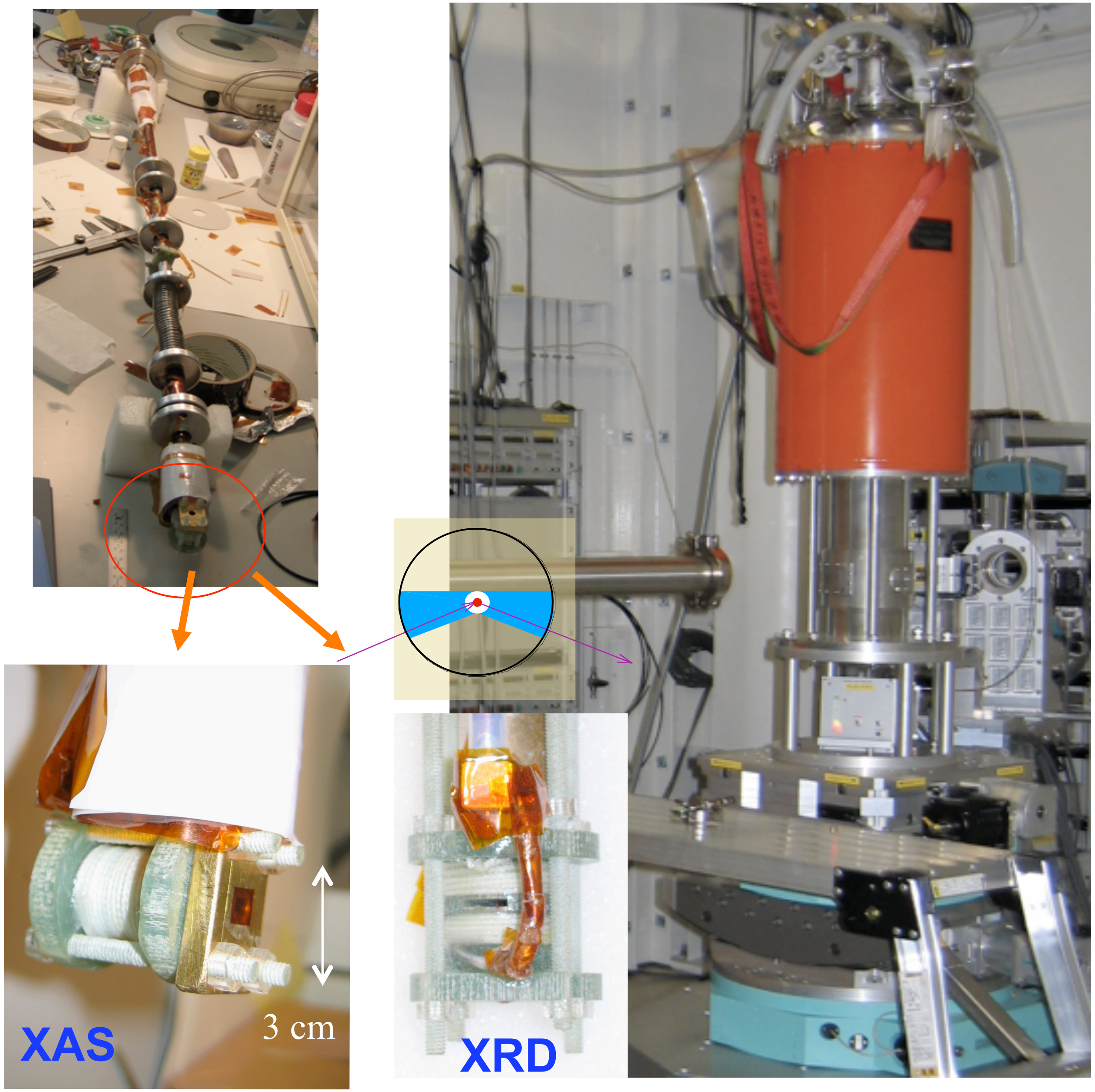

♦Low Temperature

Closed cycle He-gas refrigerator (T>10 K)

He flow cryostat (Orange Cryo.) (T> 2 K)

♦Detection

APD + MCS

PIN + Oscilloscope

2D detector (Hamamatsu C7942)

X-ray diffraction measurement

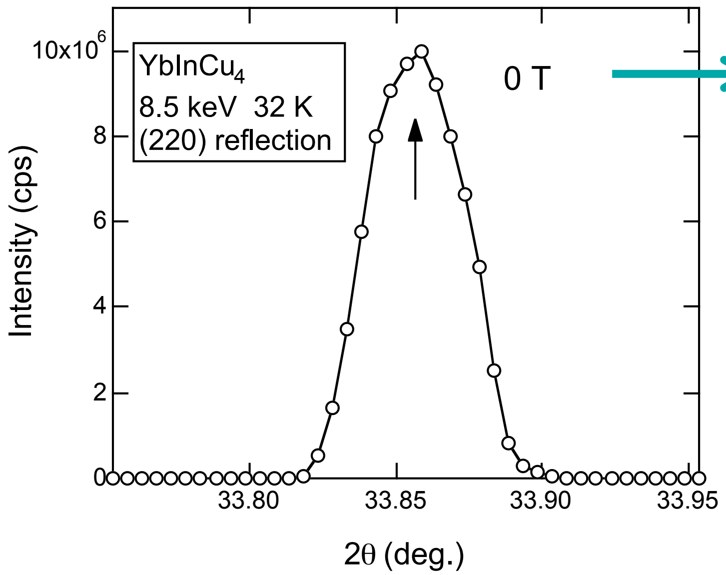

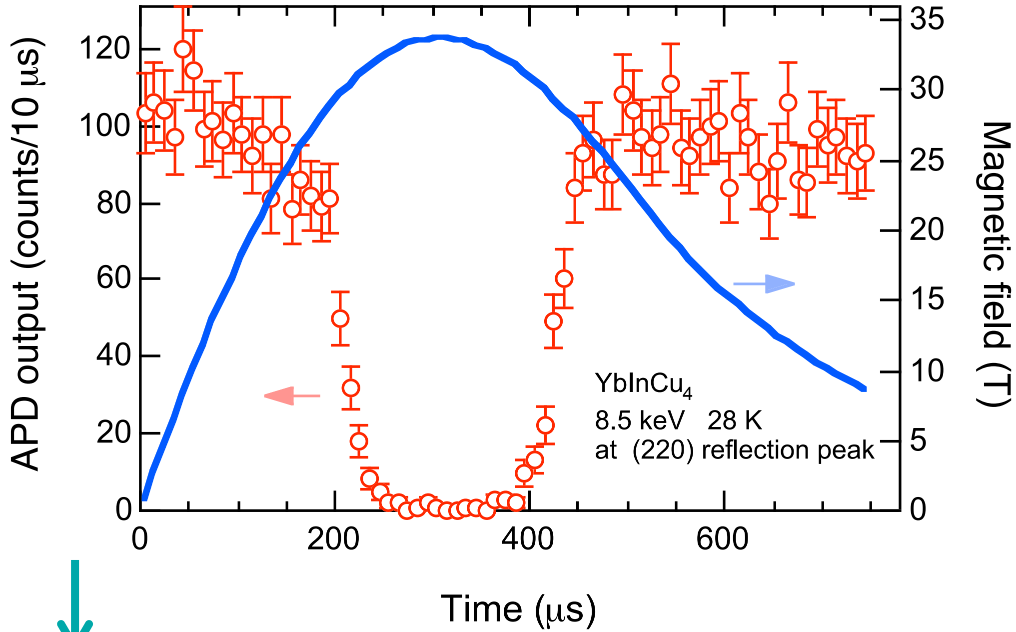

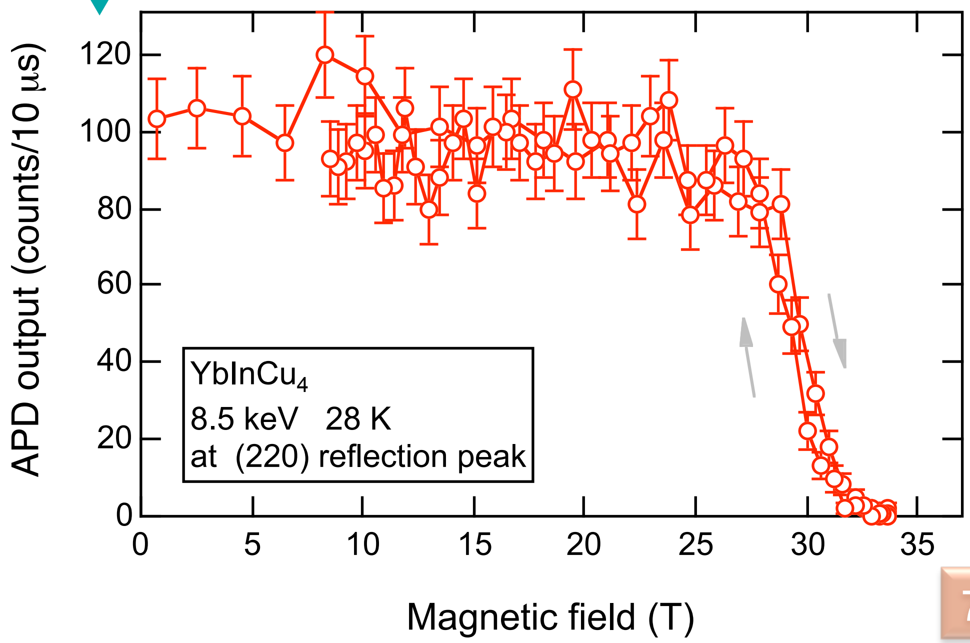

Field variation of the Bragg reflection intensity can be measured by only one shot.

$YbInCu_4$

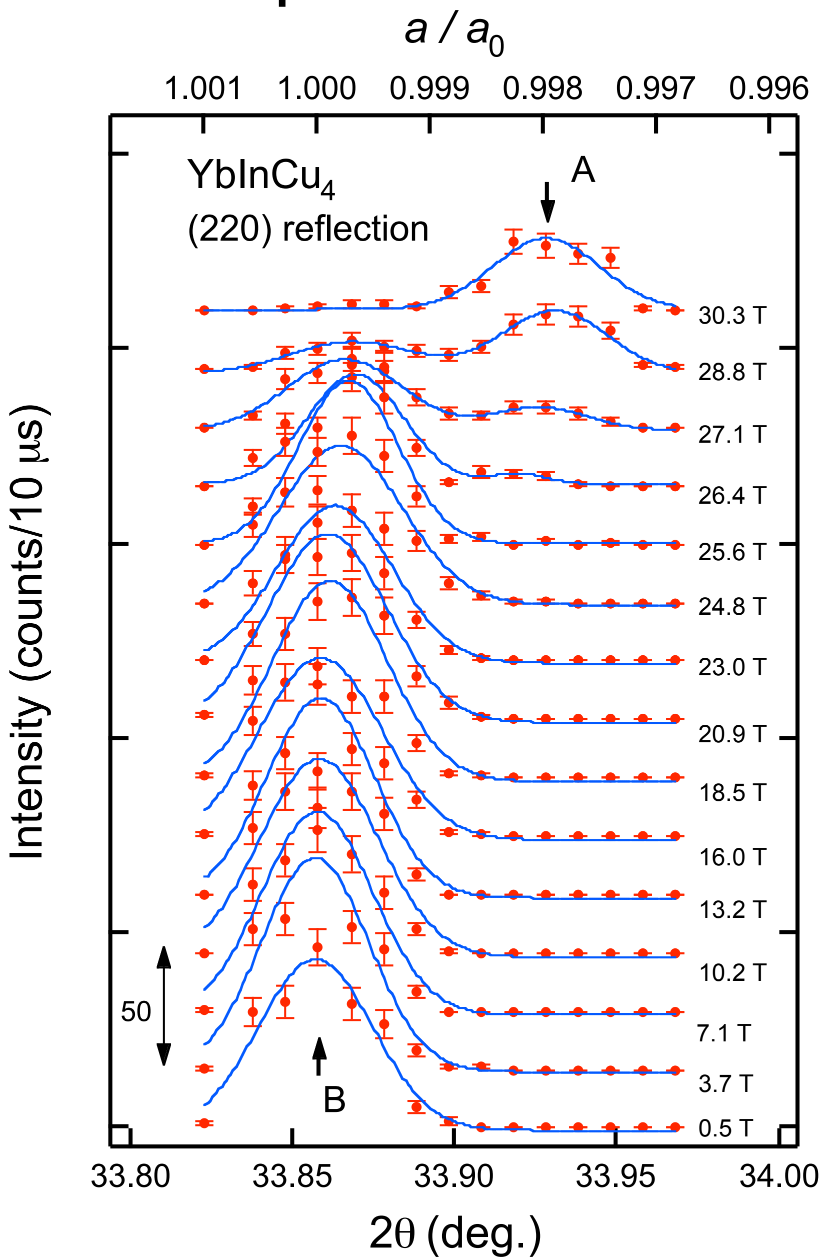

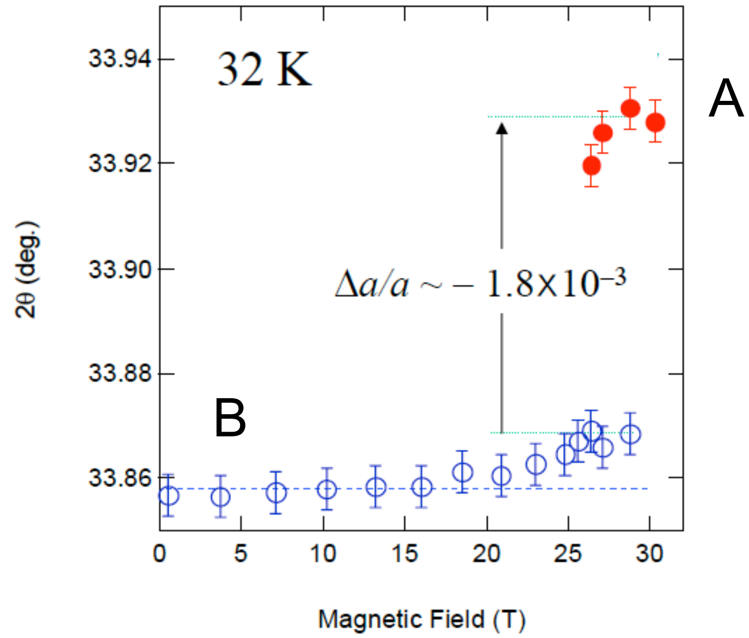

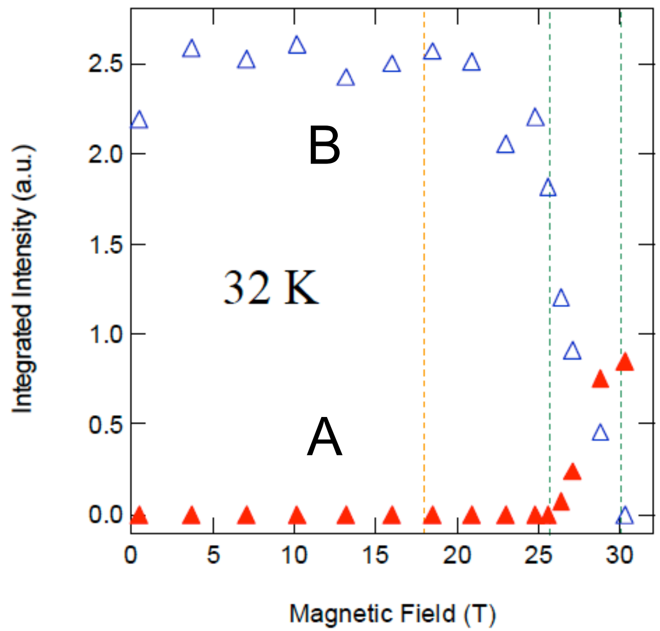

Y. H. Matsuda et al., *J. Phys. Soc. Jpn.* **75** (2006) 024710 1-5

2D-detector

$CdCr_2O_4$ T_N=8K Θ_{CW}=-70K

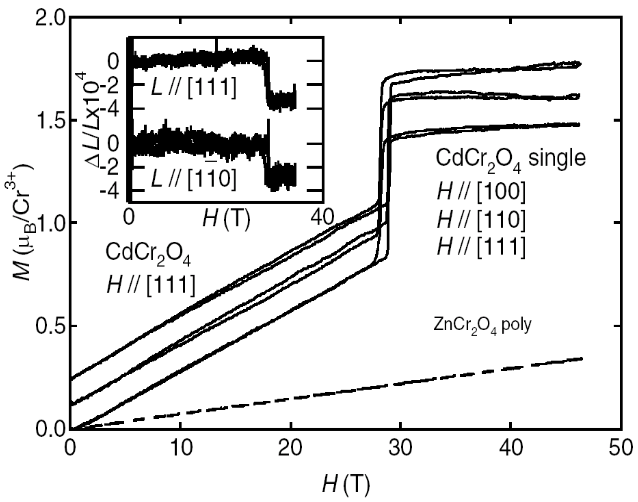

H. Ueda et al., PRL 94 (2005) 047202

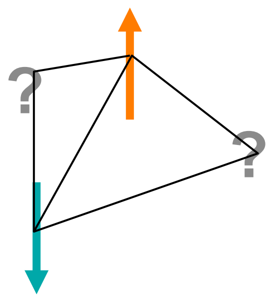

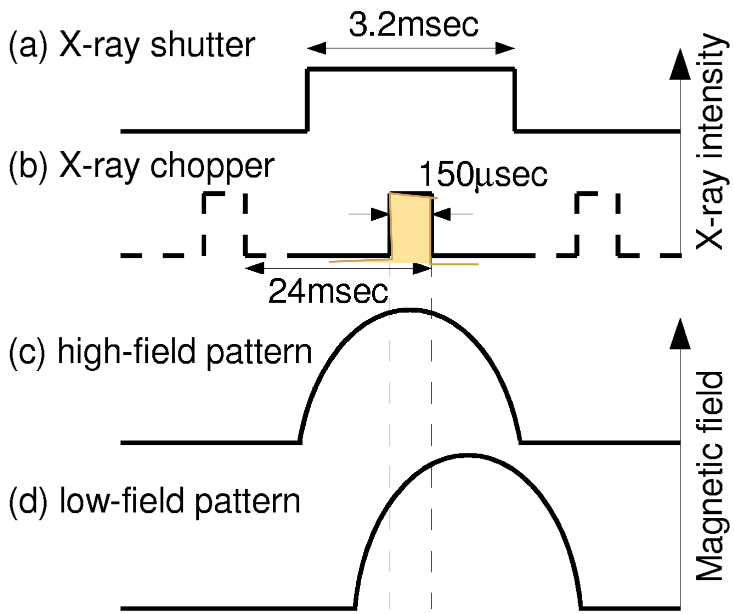

2θ 440 reflection (T=5K)

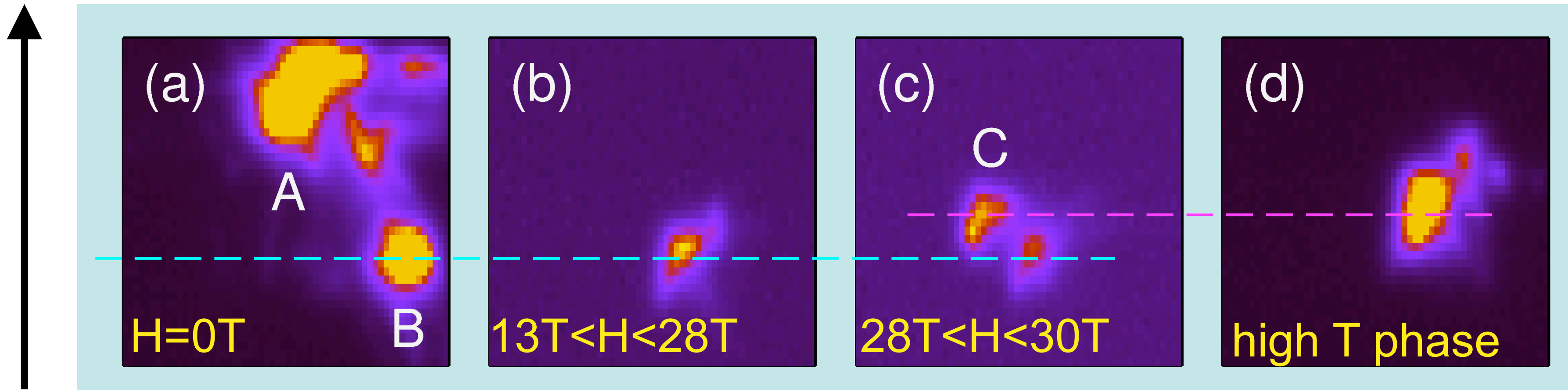

T. Inami et al., *J. Phys.: Conference Series* **51** (2006) 502-505

X-ray Absorption Spectroscopy

$EuNi_2(Si_{1-x}Ge_x)_2$

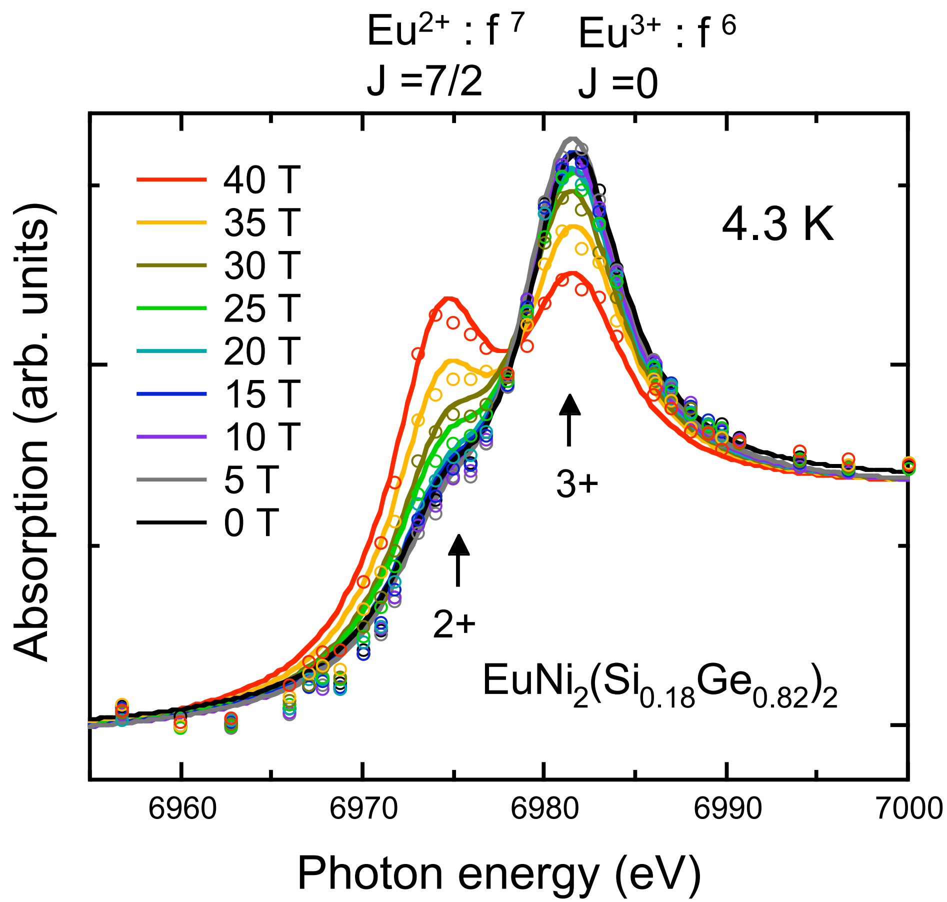

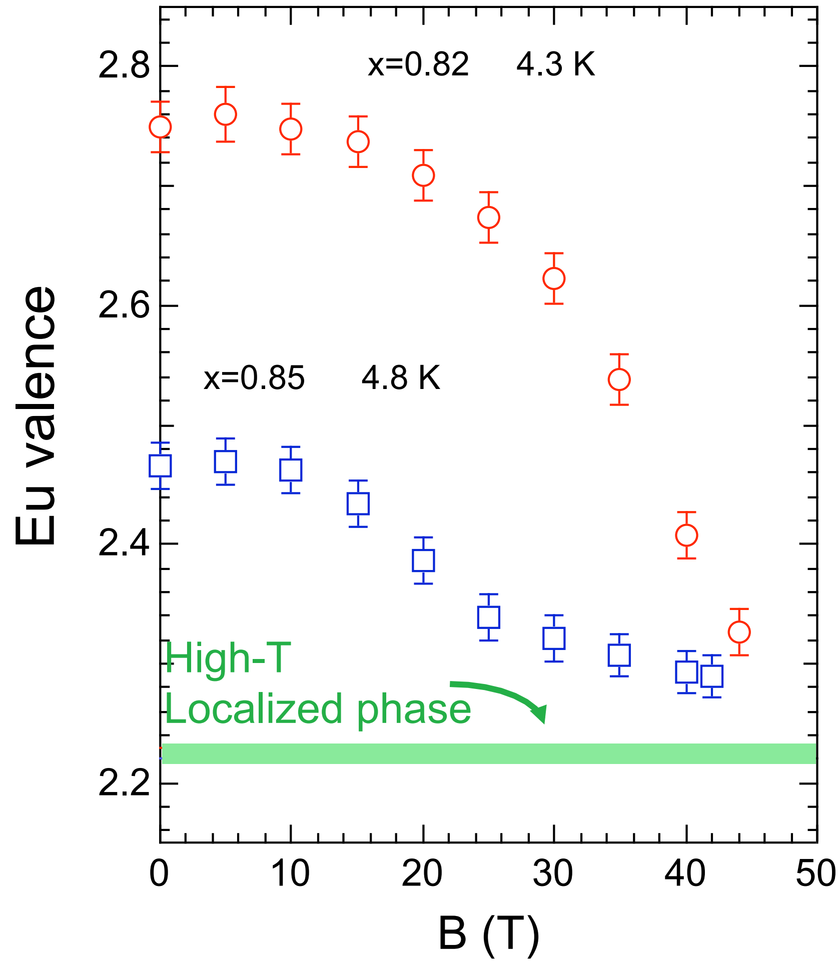

Y. H. Matsuda et al,*J. Phys. Soc. Jpn.* **77** (2008) 054713 1-7.

Y. H. Matsuda et al., *J. Phys.: Conference Series* **51** (2006) 490-493

XMCD

$\Delta\mu = \mu_+ - \mu_-$
Element and shell selective microscopic probe for magnetism

→ Powerful means for investigation of electronic states

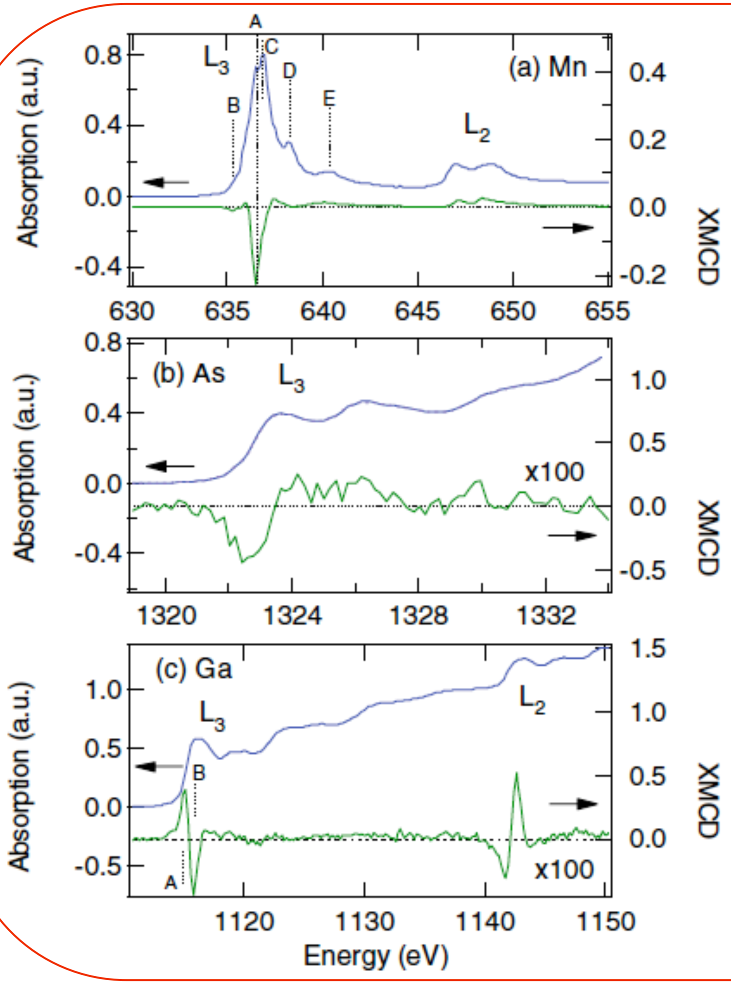

GaMnAs

D. J. Keavney et al., PRL91, (2003) 187203

Most studies were for ferromagnetic materials

using High ***B***

Field induced phenomena in antiferromagnetic and paramagnetic materials

Valence Fluctuation

Rare-earth
Intermetallic Compound

$f^n \rightleftarrows f^{n-1} + e$

Ce (f^1, f^0), Sm (f^6, f^5),
Eu (f^7, f^6), Yb (f^{14}, f^{13})

Eu^{2+} J=7/2
Eu^{3+} J=0

H. Wada et al.,
J. Phys.: Condens. Matter. **9** (1997) 7913

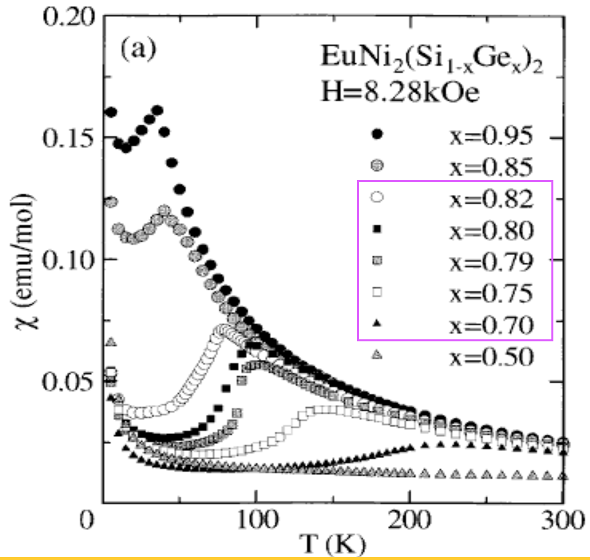

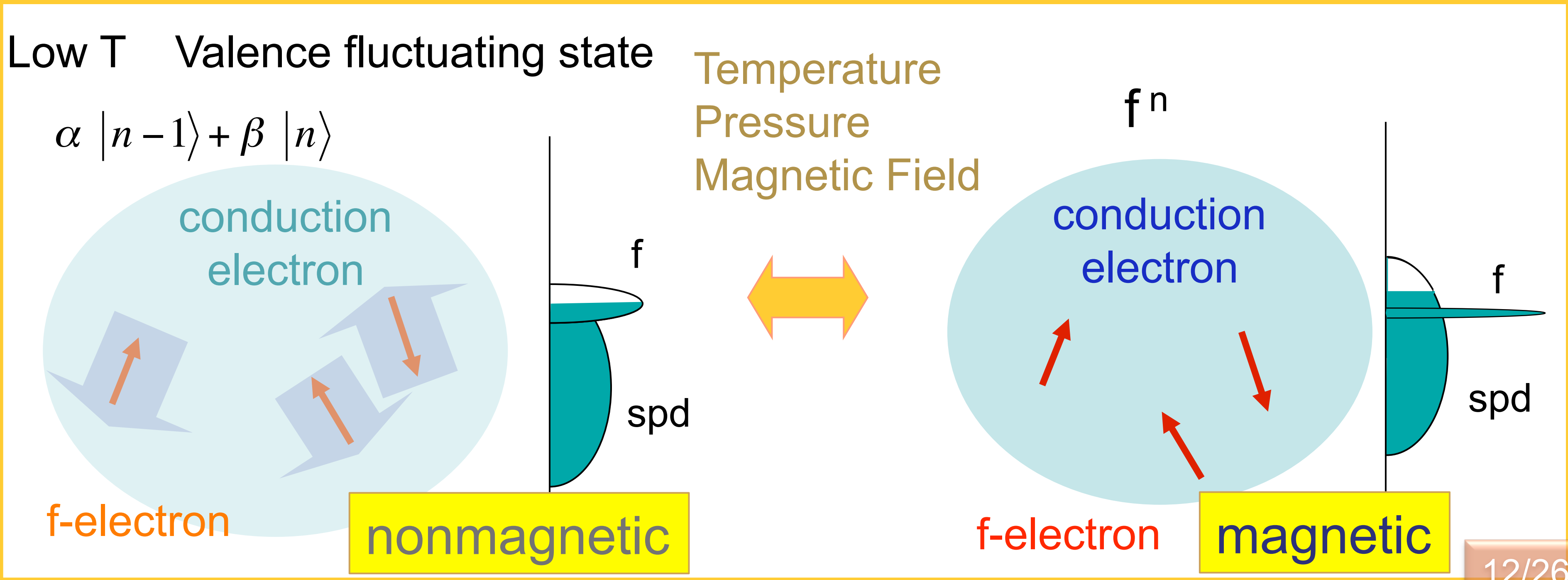

Field-induced valence transition studied by XMCD

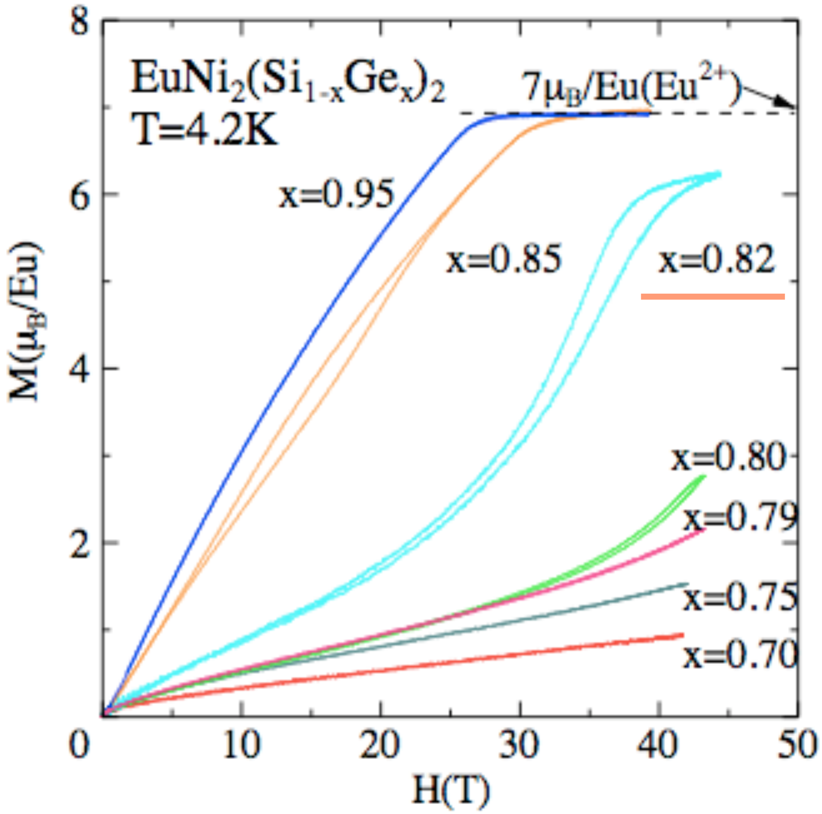

A. Mitsuda, thesis (1999) Kyoto Univ.
H. Wada, A. Nakamura, A. Mitsuda et al., J.Phys.:Condens. Matter 9 (1997) 7913.

no thermal excitation

control of electronic states

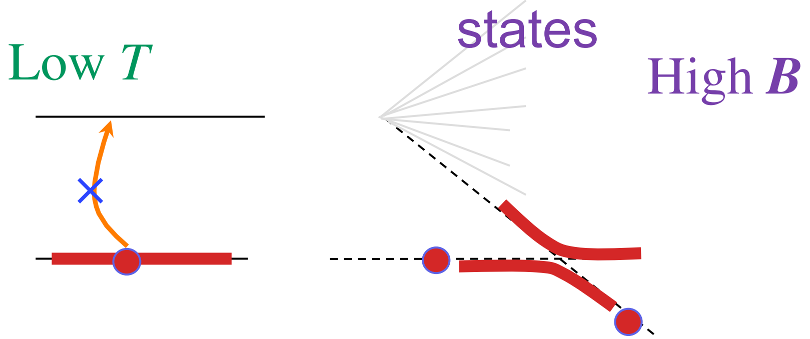

J =7/2 *J* =0

$$\alpha\left|f^{7}\right\rangle + \beta\left|f^{6}c\right\rangle$$

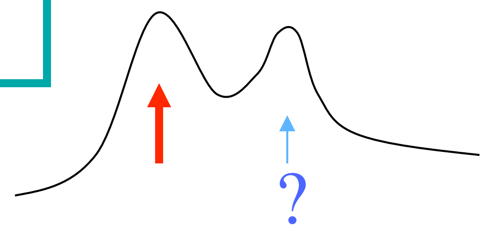

valence selectivity using x-rays

Magnetic polarization → Hybridization

Eu^{2+} (f^7, *J* =7/2) + Eu^{3+}(f^6c, *J* =0)

XMCD of $EuNi_2(Si_{0.18}Ge_{0.82})_2$

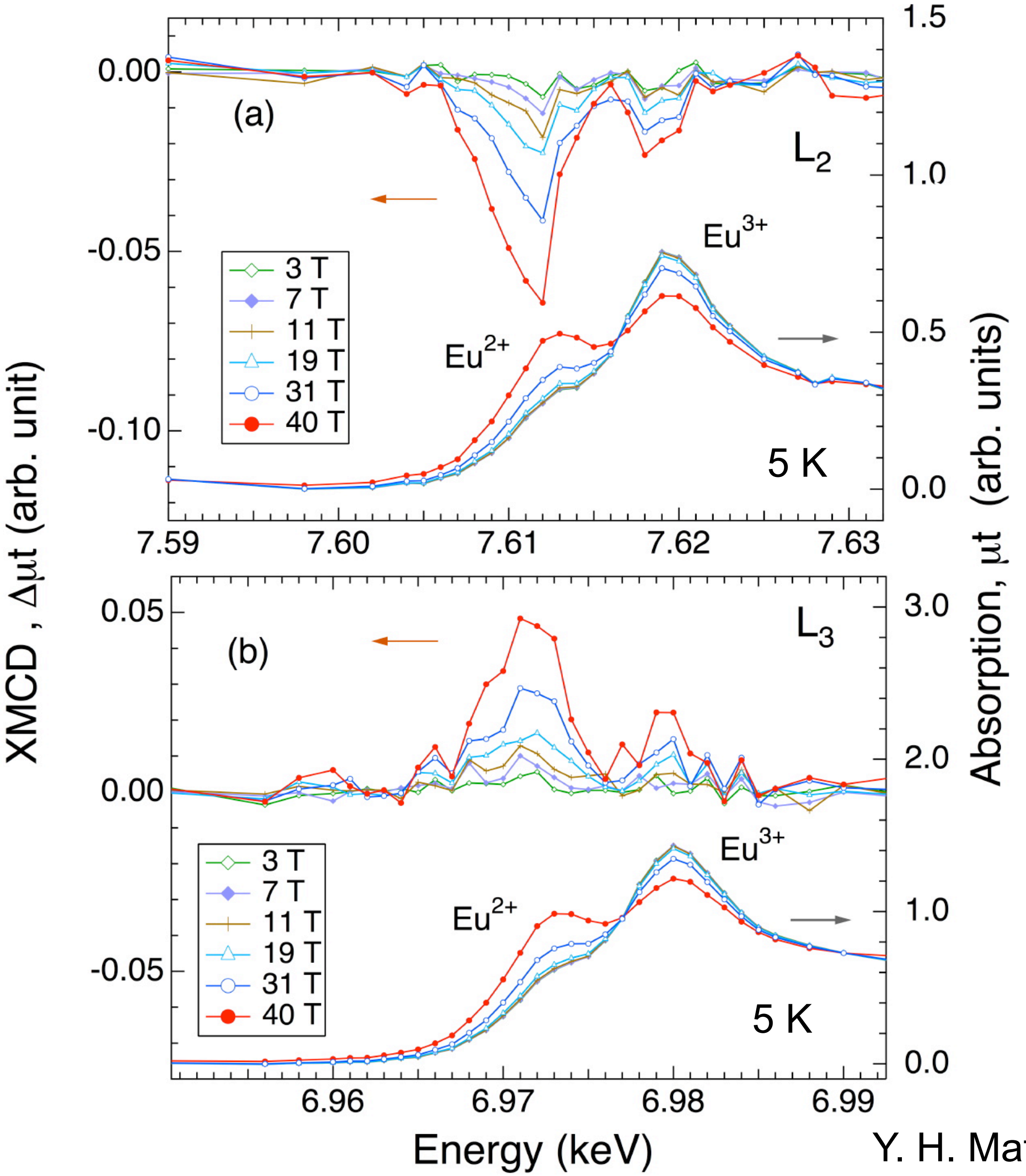

Double peak structure
Eu^{3+} (f^6 , J=0)
Eu^{2+} (f^7 , J=7/2)

L-edge *2p* → *5d*

5d electrons of Eu are magnetically polarized

Y. H. Matsuda et al.,arXiv:0901.4259 (2009)

Magnetic Filed Dependence of the XMCD intensity

Integrated XMCD peaks I_{mcd} scale together with the magnetization curve.

Degree of the magnetic polarization $P_{5d} = \frac{\int \Delta\mu t\, dE}{\int \mu t\, dE}$

Magnetic field dependence of P_{5d} is qualitatively different between Eu^{3+} and Eu^{2+} states.

$P_{5d}(3+)/P_{5d}(2+) \sim 0.1$ (B< 20 T)

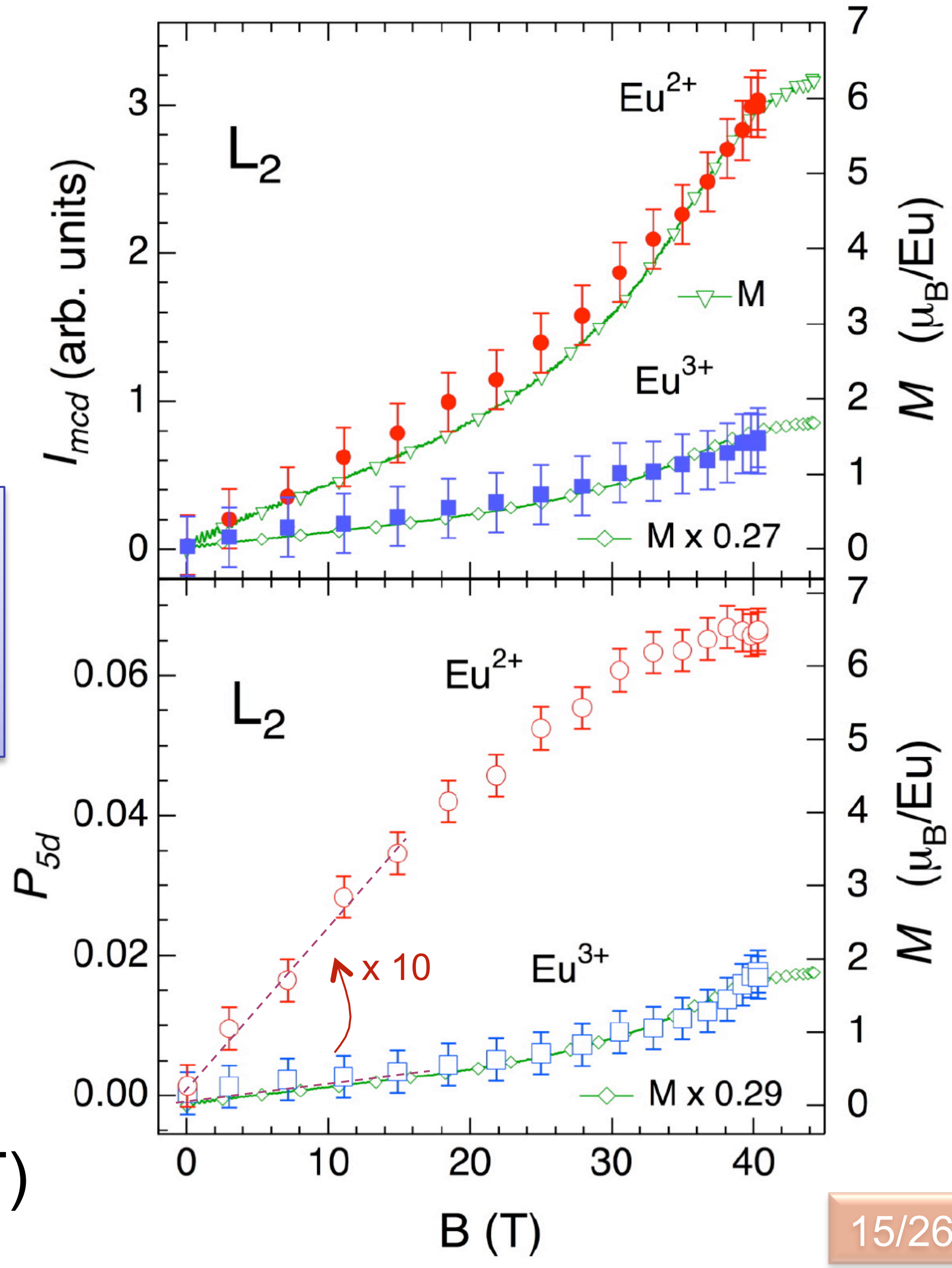

XMCD of $EuNi_2P_2$

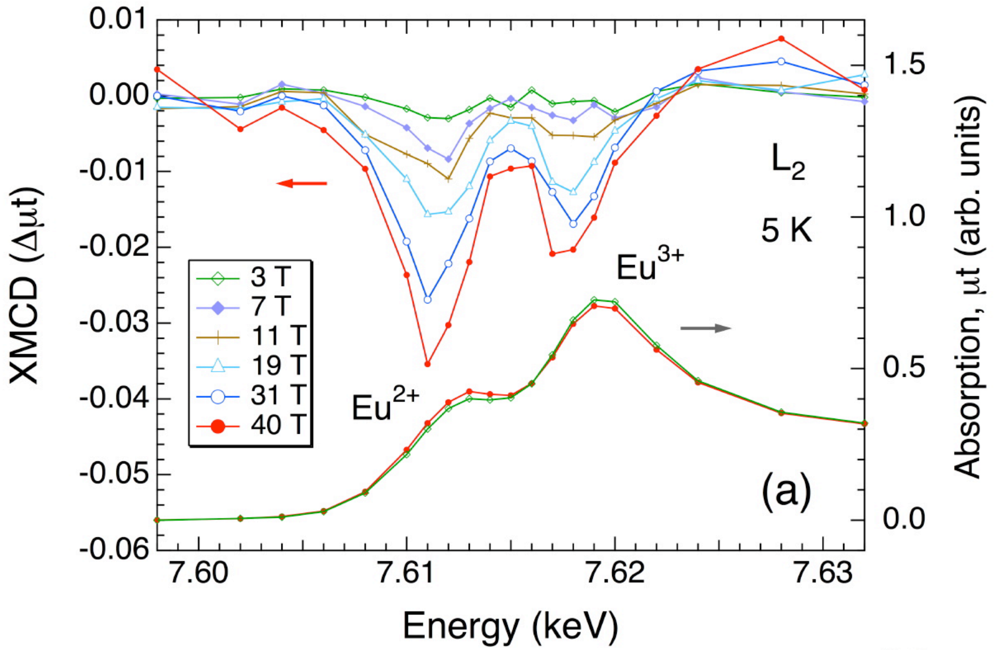

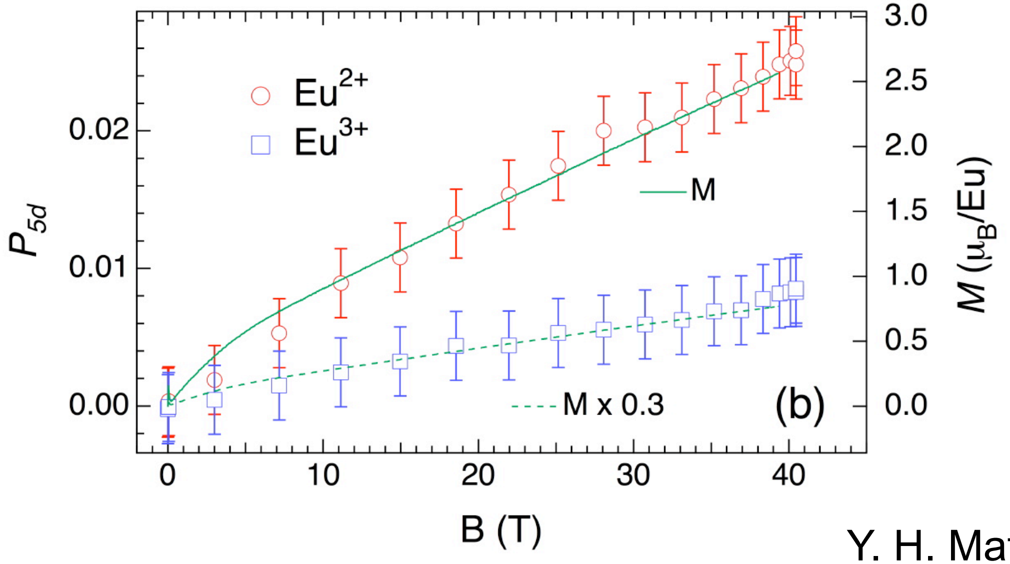

♦ Hybridization is larger than $EuNi_2(Si_{0.18}Ge_{0.12})_2$.

♦ Valence is insensitive to magnetic field.

♦ Eu^{3+}(J=0) XMCD is more significant than $EuNi_2(Si_{0.18}Ge_{0.12})_2$.

$P_{5d}(3+)/ P_{5d}(2+) \sim 0.3$

Y. H. Matsuda et al.,arXiv:0901.4259 (2009)

Discussion

1. XMCD of Eu^{3+} (f^6, J=0)

① Interference Effect

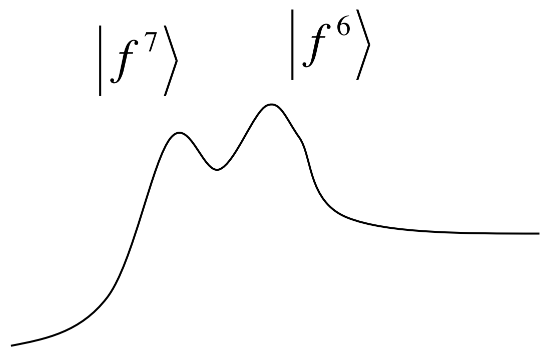

No hybridization of the final states by Coulomb repulsion due to a core hole

each absorption peak is due to the pure state

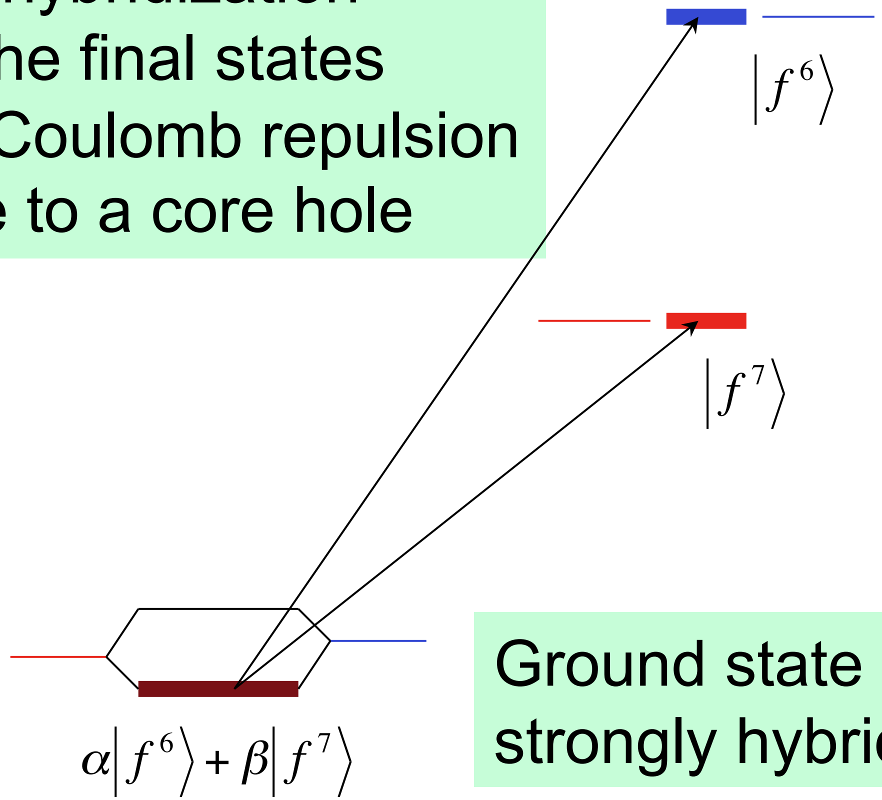

No Eu^{2+} component in the XMCD peak defined as Eu^{3+} XMCD

Ground state is strongly hybridized

② Van Vleck term

Eu^{3+}

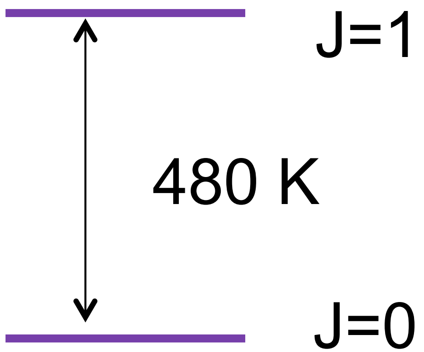

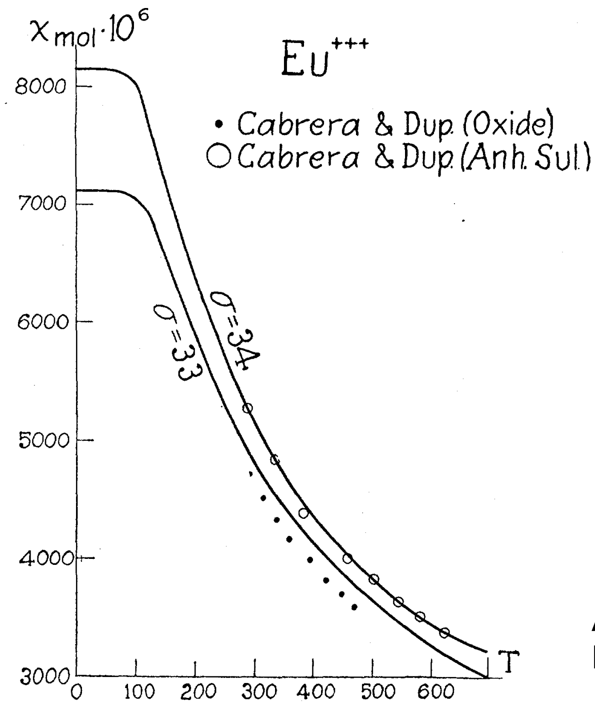

A. Frank
Phys. Rev. 39 (1932) 119.

0.3 μ_B/Eu^{3+}
at 20 T

	$EuNi_2(Si_{0.18}Ge_{0.82})_2$	$EuNi_2P_2$
$M(Eu^{3+})/M(Eu^{2+})$	0.06	0.09
$P_{5d}(Eu^{3+})/P_{5d}(Eu^{2+})$	0.12	0.30
except for the Van Vleck term	0.06	0.21

Polarization of
Eu 5d electron

③ c-f hybridization effect

c-f hybridization → conduction electrons polarized by Eu^{2+} (J=7/2)

↓

5d electrons of Eu^{3+} (J=0) are polarized by the conduction electrons

Polarization due to a local Eu^{2+} (J=7/2) state.

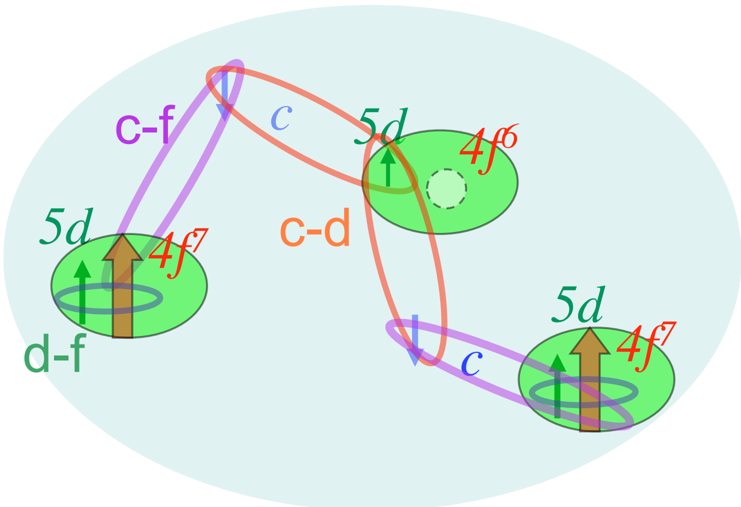

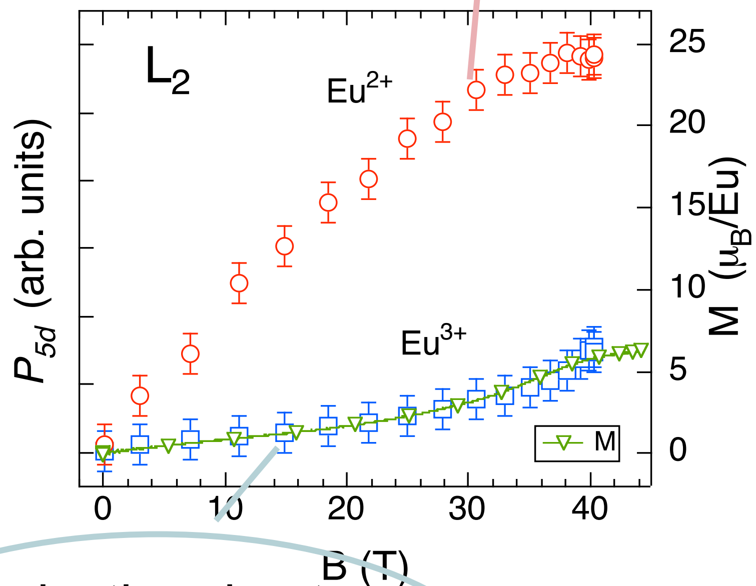

Polarization due to valence fluctuating Eu ions at neighboring sites.

Eu^{3+} MCD reflects the strength of the c-f hybridization

Y. H. Matsuda et al.,arXiv:0901.4259 (2009)

Material dependence

XMCD ⇨

	$EuNi_2(Si_{0.18}Ge_{0.82})_2$	$EuNi_2P_2$
$P_{5d}(Eu^{3+})/P_{5d}(Eu^{2+})$	0.06~0.12	0.21~ 0.30

× 3.5~2.5

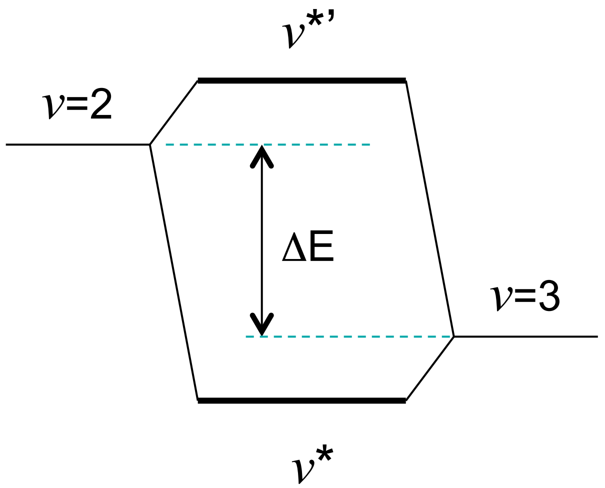

	$EuNi_2(Si_{0.18}Ge_{0.82})_2$	$EuNi_2P_2$
Low T, zero field		
Eu valence ν^*	2.8	2.6
V	0.7ΔE	2.3ΔE

× 3.3

$V = -\langle \nu=2|\mathcal{H}|\nu=3\rangle$

Hybridization parameter

P_{5d} of Eu^{3+} ⇨ strength of the hybridization

DXAFS : PF-AR NW2A (KEK Tsukuba)

Photon Factory AR　NW2A

DXAFS spectrometer

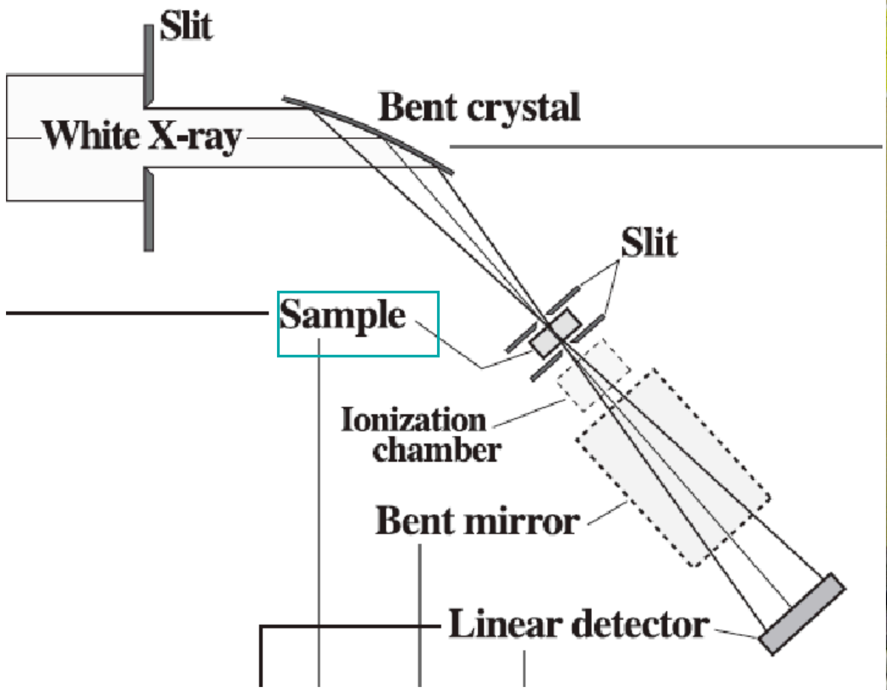

Y. Inada、M. Nomura
Photon Factory News
vol. 23 No.1(2005)

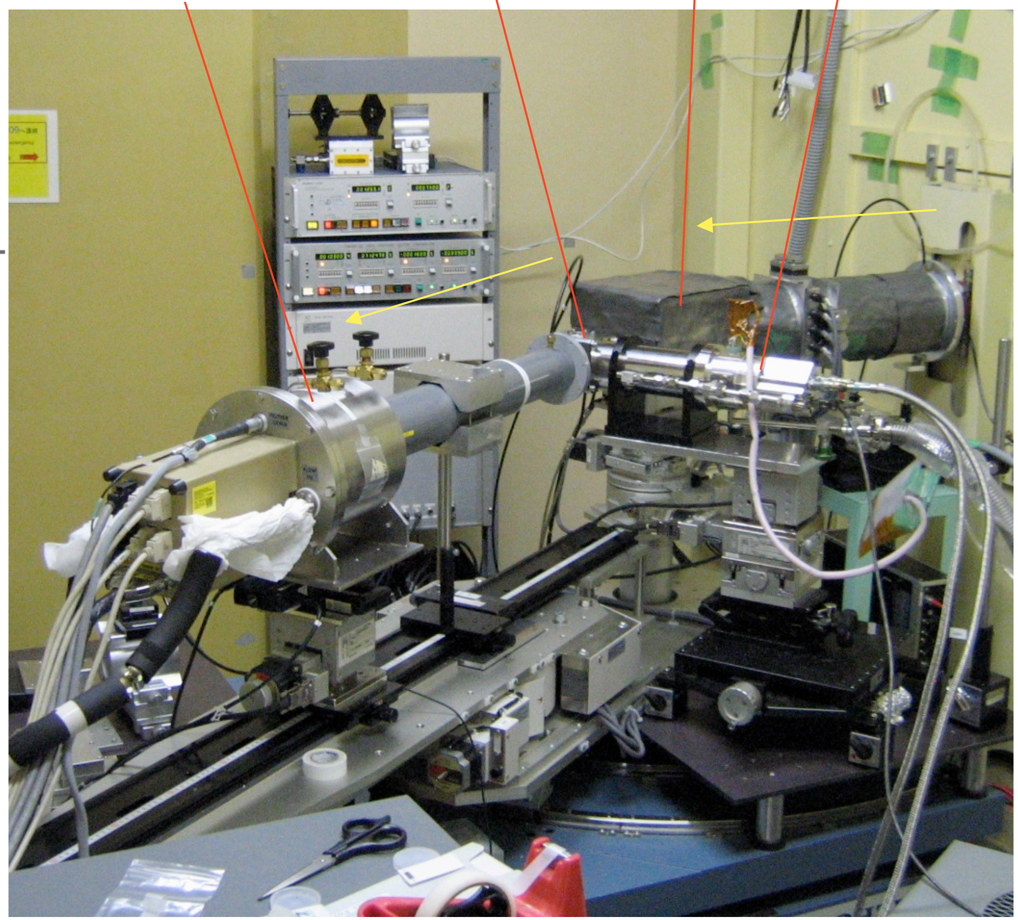

High-Magnetic-Field DXAFS Study

Gate Δt = 100 μs

$Pr_{0.6}Ca_{0.4}MnO_3$ Field-induced Insulator−Metal transition

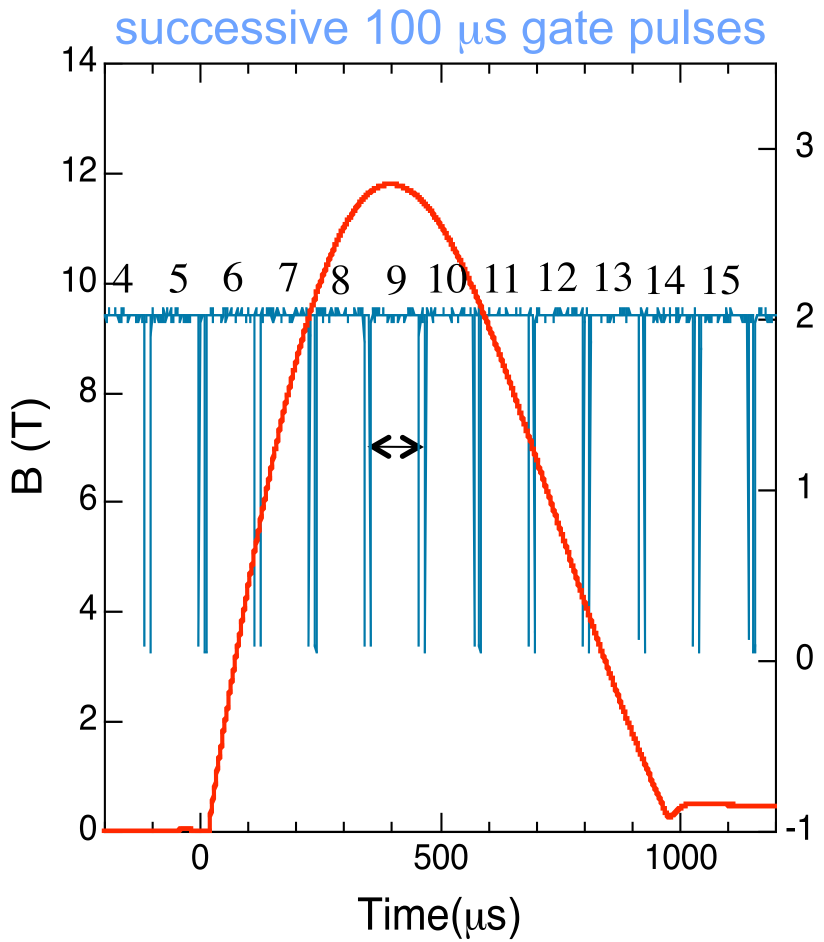

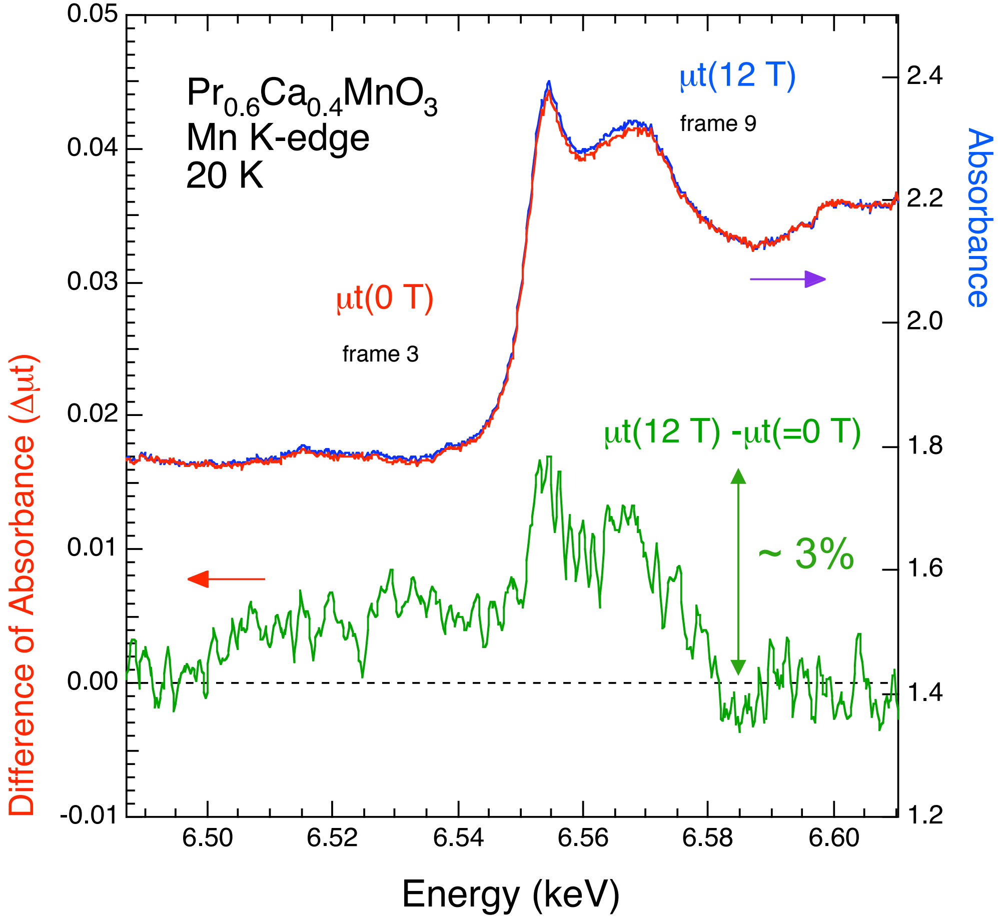

A small absorption change due to the field-induced I-M transition is detected.

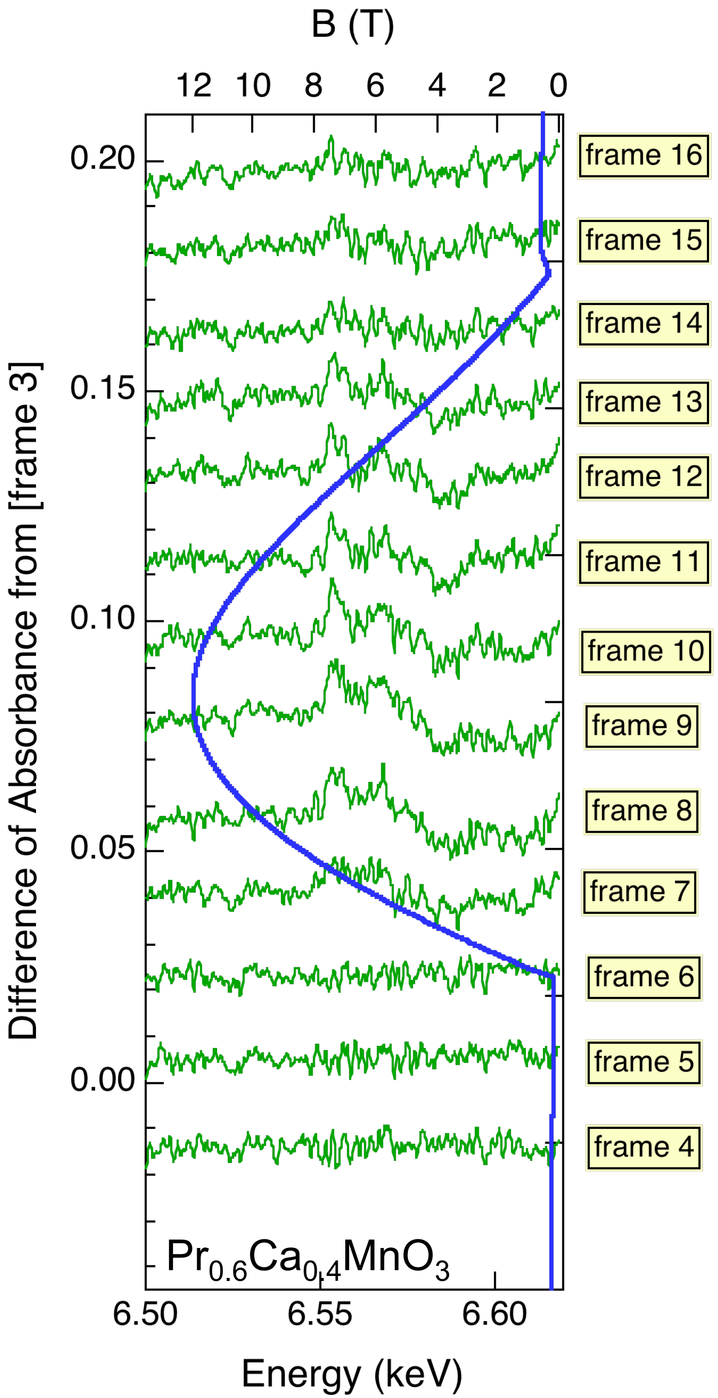

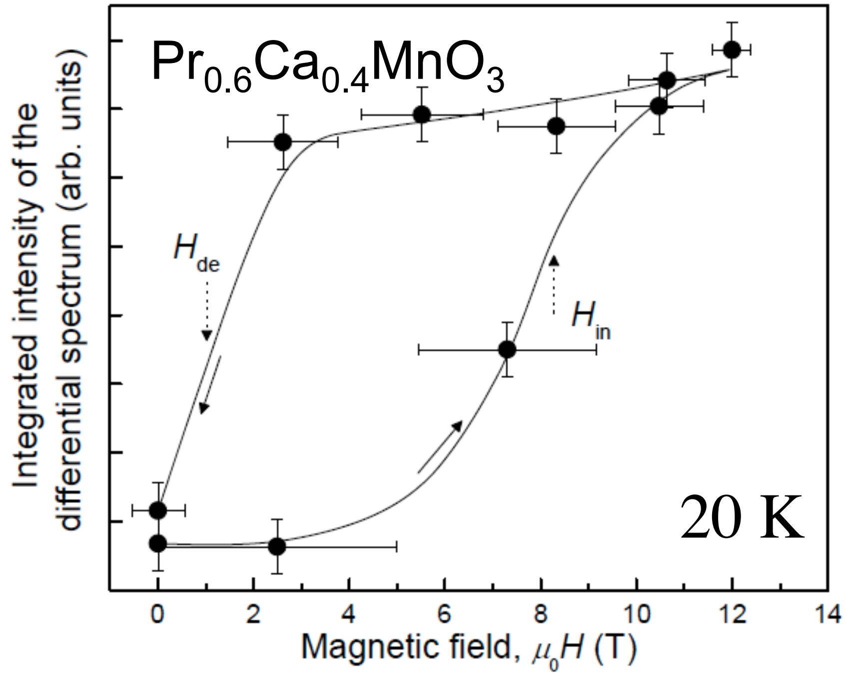

Z. W. Ouyang, Y. H. Matsuda, et al.,
J. Phys. : Condens. Matter **21** (2009) 016006.

Development of techniques underway

- Pulsed magnet & Cryostat

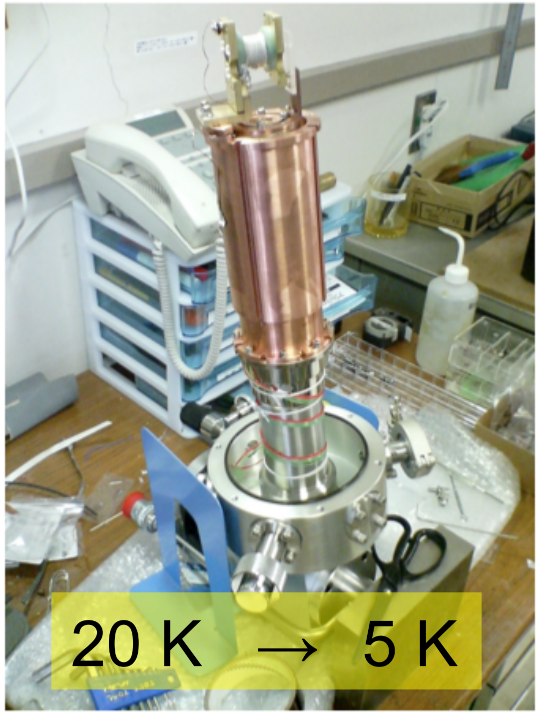

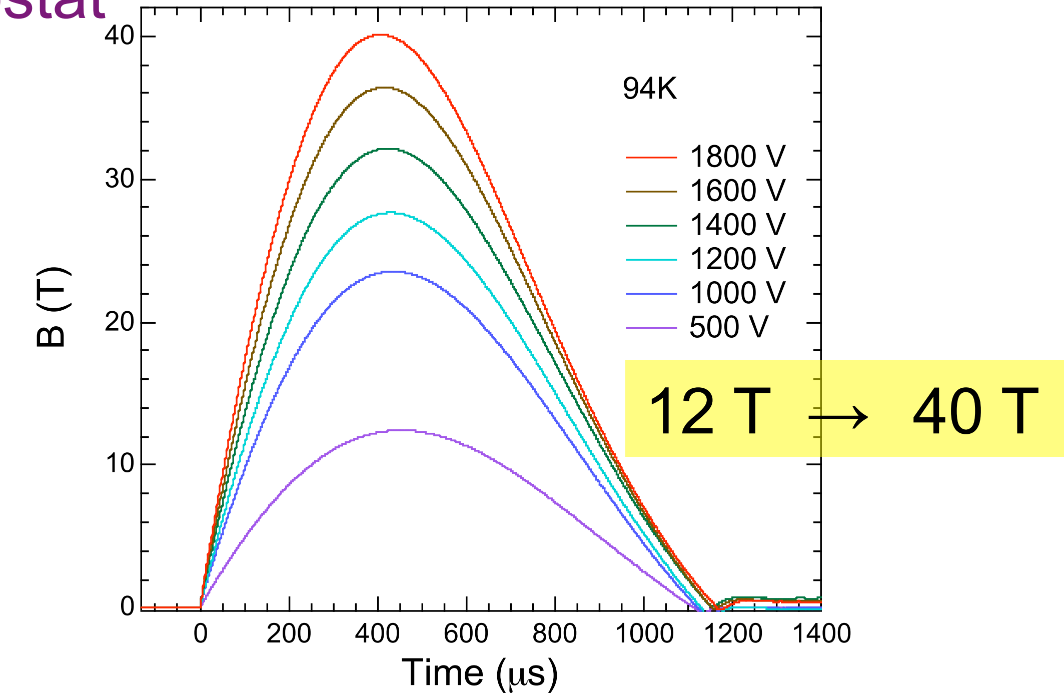

- A diamond phase retarder for XMCD

in collaboration with
K. Hirano (KEK-PF)

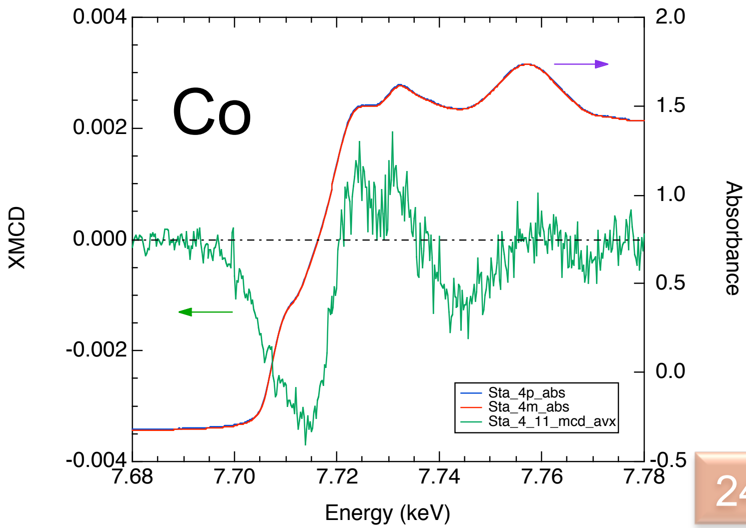

Summary

- Valence selective XMCD in $EuNi_2(Si_{1-x}Ge_x)_2$ and $EuNi_2P_2$ were measured up to 40 T using a mini-magnet.

- XMCD of Eu^{3+} (J=0) possibly reflects the magnetism of itinerant states through the c-f hybridization, while XMCD of Eu^{2+} (J=7/2) reflects localized states.

- DXAFS experiment in high magnetic fields were made. At the field-induced I-M transition of $Pr_{0.6}Ca_{0.4}MnO_3$, recovering the local lattice distortion induces an enhancement of the Mn K-edge absorption intensity.

Other collaborators

Y. Murakami (Tohoku Univ.) Discussions

K. Yoshimura (Kyoto Univ.) $YbInCu_4$

A. Mitsuda (Kyushu Univ.) $EuNi_2(Si_{1-x}Ge_x)_2$

H. Ueda (Univ. Tokyo) $CdCr_2O_4$

T. Matsumura (Hiroshima Univ.) TbB_4

T. Arima (Tohoku Univ.) $Pr_{0.6}Ca_{0.4}MnO_3$

M. Suzuki, N. Kawamura (JASRI/SPring-8)

XMCD / BL39XU

Y. Inada, Y. Niwa, M. Nomura (KEK PF)

DXAFS / PF-AR NW2A